Hydrodynamic Chromatography

André M. Striegel[1] and Amandaa K. Brewer[2]

[1]Analytical Chemistry Division, National Institute of Standards and Technology, Gaithersburg, Maryland 20899; email: andre.striegel@nist.gov

[2]Tosoh Bioscience LLC, King of Prussia, Pennsylvania 19406; email: amandaa.brewer@tosoh.com

Annu. Rev. Anal. Chem. 2012. 5:15–34

The *Annual Review of Analytical Chemistry* is online at anchem.annualreviews.org

This article's doi:
10.1146/annurev-anchem-062011-143107

1936-1327/12/0719-0015$20.00

Keywords

multiple detection, particle sizing, polymer characterization, chromatography fundamentals, packed-column HDC, microcapillary HDC

Abstract

Hydrodynamic chromatography (HDC) has experienced a resurgence in recent years for particle and polymer characterization, principally because of its coupling to a multiplicity of physical detection methods. When coupled to light scattering (both multiangle static and quasi-elastic), viscometric, and refractometric detectors, HDC can determine the molar mass, size, shape, and structure of colloidal analytes continuously and as a function of one another, all in a single analysis. In so doing, it exposes the analytes to less shear force (and, hence, less potential for flow-induced degradation) than in, for instance, size-exclusion chromatography. In this review, we discuss the fundamental chromatographic underpinnings of this technique in terms of retention, band broadening, and resolution, and we describe the power of multidetector HDC with examples from the recent literature.

1. INTRODUCTION

Numerous processing and end-use properties of colloidal matter, both macromolecular and particulate, depend on structural properties such as size, shape, and compactness, among others. Moreover, in all synthetic and many natural colloids, these structural properties have a distribution that ranges from narrow and monomodal to broad (possibly covering several orders of magnitude) and multimodal. Accurate determination of these distributions is essential in the design and synthesis of new materials, as well as for optimizing processing conditions and for effectively tailoring end-use functions. For example, the distributions of particle size and shape affect solid-state properties such as powder packing, abrasive efficiency, friction, and bulk density of materials. They also affect solution- and melt-state rheological properties such as drag; mixing; and viscosity of solutions, suspensions, and melts.

For the purposes of this review, we consider a particle to be an object with some linear dimension between 100 Å (10 nm or 0.01 μm) and 100,000 Å (10,000 nm or 10 μm). As shown in **Figure 1*a***, this description covers a wide range of natural and synthetic materials. Additionally, the term ultrahigh molar mass generally denotes macromolecules with molar mass $M \geq 1 \times 10^6$ g mol^{-1}, although, as described below, we deal with polymers and particles with M that greatly exceeds this threshold. As mentioned above, in a given sample the size range of the analyte of interest may span several orders of magnitude, and across this range, the shape, compactness, and chemistry of the analyte may also vary. As such, the holy grail of particle sizing may be understood as (*a*) the accurate and precise determination of the particle-size averages and distribution of a sample that is polydisperse in size, shape, structure, and chemistry and (*b*) the determination of the averages, distributions, and mutual interdependences of all these properties (i.e., How does shape vary as a function of size? How does structure vary as a function of size and shape?).

As shown in **Figure 1*b***, numerous analytical techniques have been developed to measure particle size over the range presented in **Figure 1*a***. Although each technique has advantages and limitations, a discussion of the individual methods is beyond the scope of the present article. Excellent recent reviews may be found in References 1 and 2. Here, we focus on a particular method that covers a broad swath of the size range depicted in **Figure 1** and that has experienced

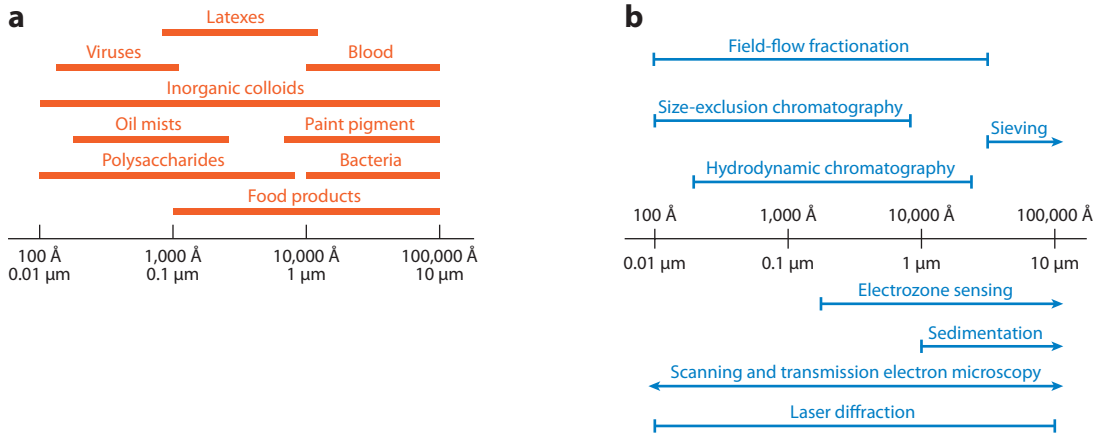

Figure 1

(*a*) Typical particles with dimensions between 100 Å (0.01 μm) and 100,000 Å (10 μm). (*b*) Typical particle-sizing methods and applicable ranges.

a resurgence in recent years, principally because of its coupling to a multiplicity of detection methods. This technique is hydrodynamic chromatography (HDC).

HDC is a solution-phase separation method that can be performed in an open tube (capillary) or in a column packed with nonporous, inert particles (as we discuss below, packing particles with very small pores, vis-à-vis the solution size of the analyte, can also be employed). In HDC, sample components are segregated in a size-dependent manner on the basis of preferential sampling of the streamlines of flow in the capillary or in the interstitial medium of the packed column. Such segregation is the first step in characterizing size averages and distributions. Coupling HDC to various detection methods further informs our knowledge of analyte shape and structure and of the dependence of these features on size as a continuous function of the latter.

In this review, we first cover, with broad strokes, the historical development of HDC, then delve more fully into fundamental aspects of the technique, namely descriptions of the mechanism of retention and of factors affecting band broadening and resolution. Finally, we show via examples from the recent literature the power of multidetector HDC for characterizing complex particles and ultrahigh-*M* polymers, and we also highlight recent developments in the area of capillary HDC.

HDC: hydrodynamic chromatography

HSA: human serum albumin

SBF: separation by flow

SEC: size-exclusion chromatography

2. HISTORICAL DEVELOPMENT OF HYDRODYNAMIC CHROMATOGRAPHY

The first reported separation to proceed via an HDC-type mechanism and to have been recognized as such appears to be that described in 1962 by Pedersen (3), who fractionated a mixture of the proteins *Helix* hemocyanin and human serum albumin (HSA) on a column packed with 20- to 35-μm impermeable glass spheres. Having ruled out sorptive effects, and even though chromatographic resolution was quite low, Pedersen showed that separation had indeed occurred by monitoring two different wavelength-of-absorption ratios and by noting the preferential enrichment of hemocyanin in one portion of the peak and of HSA in another portion. Because of the particular experimental setup, the author deduced that separation must have been caused by flow in the interstitial medium, that is, in between the column packing particles. Pedersen suggested an explanation for this observation that was based on an analogy to the flow of blood cells through blood vessels; however, because in the latter scenario flow appears to be controlled chiefly by tubular pinch effects, this explanation was deemed too restrictive with respect to subsequent observations and calculations by other authors.

In a series of papers beginning in 1969, DiMarzio & Guttman (4–7) laid out the theoretical foundations of a technique that they termed separation by flow (SBF) and that is now generally recognized as HDC. These authors explained the means by which separation of particles and macromolecules may occur in an open tube or in the interstitial medium of a packed column. They also examined the effects of Fickean versus non-Fickean diffusion and of capillary geometry (e.g., a circular versus triangular or other cross section); proposed figures of merit, conditions for optimal separation, and criteria of resolution; examined band-broadening effects; and proposed how to calculate the effective size of flexible macromolecules by this technique. Except, perhaps, for trying to employ the SBF mechanism to explain separation in size-exclusion chromatography (SEC), in which separation is now recognized as occurring by a different mechanism (8), DiMarzio & Guttman's research is seminal in the field, and their calculations and conclusions still hold up quite well. (Note that HDC effects may occur during SEC separations. This point is explored further in Section 8.1.)

In their first 1970 paper, DiMarzio & Guttman (5) noted that "[t]he question naturally arises as to whether the separation by flow phenomenon is of any practical use. . . . [T]his can be answered

PS: polystyrene

THF: tetrahydrofuran

MMD: molar mass distribution

VISC: viscometry

DRI: differential refractometry

MALS: multiangle static light scattering

SC: slalom chromatography

QELS: quasi-elastic light scattering (also known as dynamic light scattering or photon correlation spectroscopy)

only by construction of a working instrument based on the phenomenon." They did not have long to wait for experimental confirmation of their work: In 1974, Small (9) published the first experimental paper on HDC. The apparatus built by Small employed a series of packed columns to separate and determine the particle size of various polystyrene (PS) latexes, as well as of styrene-butadiene latexes, carbon black, and colloidal silica. He proposed a separation mechanism based on the work of DiMarzio & Guttman; examined experimental aspects such as elution dependence on column packing type and size and on ionic strength of the eluent; compared latex diameters obtained by HDC by using a calibration curve to diameters obtained by electron microscopy and light scattering; employed the method to measure particle growth kinetics during emulsion polymerization; and noted the deposition (mechanical entrainment) of 0.5-μm PS latexes on the HDC column bed, a phenomenon still encountered to this day and for which a proper explanation has not yet been put forth.

In a series of papers published mostly during the 1990s, Tijssen, Kraak, and coworkers explored many of the chromatographic underpinnings of HDC (10–17). Rather than discuss their findings at this point, in a historical context, we do so in the context of retention, band broadening, and resolution in HDC (Sections 3–5). Of particular note, however, is the 1991 publication by Stegeman et al. (12), who demonstrated HDC separation with an SEC column. A series of narrow dispersity PS standards dissolved in tetrahydrofuran (THF) at room temperature and ranging in weight-average molar mass (M_w) from 2.2×10^3 to 4.0×10^6 g mol^{-1}, and also toluene, were analyzed on an SEC column with an exclusion limit of $\sim 5.0 \times 10^4$ g mol^{-1} (based on PS in THF at room temperature). Elution by a strict SEC mechanism should have caused all the analytes with $M > 5.0 \times 10^4$ g mol^{-1} to elute together at the exclusion volume of the column, as these analytes are too large to penetrate the pores of the column packing material and thus sample only the interstitial volume of the column. This expected coelution did not happen. Rather, separation of all analytes with $M > 5.0 \times 10^4$ g mol^{-1} occurred by an HDC mechanism that operates in the interstitial medium of the column.

The above result obtained by Stegeman et al. has two important consequences. First, depending on the pore size of the column packing material and on the size range of the sample, both SEC and HDC may occur during a separation with an SEC column (discussed further in Section 8.1). Second, HDC experiments may be conducted with an SEC column, especially if the size of all components in the sample is larger than that of the largest pores in the column packing material. The latter observation allows the large commercial offering of aqueous and organic SEC columns to potentially be converted into HDC columns.

As with SEC, the true power of HDC is generally best harnessed via a multidetector approach. The use of dual-detector HDC goes back at least to the mid 1980s, when Langhorst et al. (18) coupled low-angle static light scattering and UV detection to HDC to determine the molar mass distribution (MMD) of nonionic and partially hydrolyzed polyacrylamide. Dual-detector studies conducted over the next two decades included the online coupling of differential viscometry (VISC) and differential refractometry (DRI) to HDC to study PS latexes (19); dual-angle static light scattering and DRI in the study of waxy maize starch (20); and multiangle static light scattering (MALS) and UV detection to study the coil-stretch transition in polymers and the transition from an HDC mode to a slalom chromatography (SC) mode of elution within a column (21, 22).

More recently, Brewer & Striegel (23–29) ushered in the era of multidetector HDC with their triple- and quadruple-detector research on characterizing the mutual interdependences of molar mass, size, shape, and structure of various analytes, including broadly disperse colloids and ultrahigh-M polysaccharides. Some results from this work, which included the use of on-line MALS, VISC, DRI, and quasi-elastic light scattering (QELS) detection, are reviewed in Section 6.

In tandem with developments in multidetector HDC, numerous recent groundbreaking studies have signaled the resurgence of microcapillary HDC. This research, which has focused on the study of DNA and DNA fragments, is certain to generate increasing interest in the bioanalytical arena; it is reviewed in Section 7.

3. RETENTION IN HYDRODYNAMIC CHROMATOGRAPHY

HDC is a solution-phase liquid chromatographic separation method in which the dissolved sample is injected into an open tube, a column packed with solid beads, or a column packed with porous beads of pore size substantially smaller than the size of the analytes in solution. In packed-column HDC, the beads should be inert, that is, made of a material that minimizes non-HDC enthalpic interactions between the beads and the dissolved analytes. Such non-HDC effects can be minimized through the addition of salts and/or surfactants to the solvent/mobile phase to screen electrostatic and van der Waals interactions, which are especially common in aqueous media (30).

Separation in HDC arises from the parabolic or Poiseuille-like flow profile that develops, under laminar flow conditions, in an open tube (**Figure 2*a***) or in the interstitial medium of a packed column (**Figure 2*d***), where the fastest streamlines of flow are in the middle of the tube (or the interstitial medium) and the slowest are near the walls (or the packing particles). The center of mass of the larger analytes in the sample cannot approach the walls of the tube (or the packing particles) as closely as the center of mass of the smaller analytes can (**Figure 2*b***). As such, larger analytes remain near the center of the flow profile, where they preferentially experience faster streamlines and travel through the tube (packed column) with the average velocity of these streamlines. The

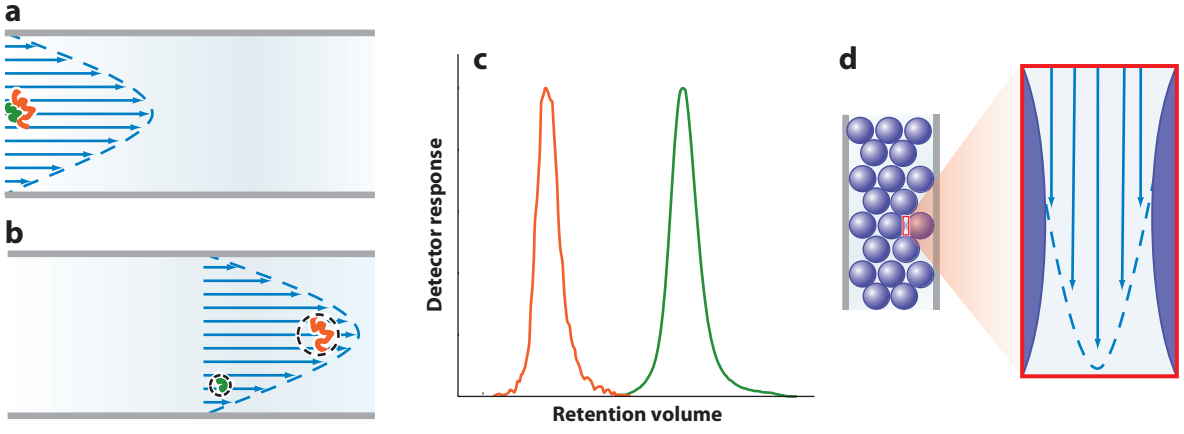

Figure 2

Mechanism of separation in hydrodynamic chromatography (HDC). Arrows indicate the streamlines of flow. (*a*) A two-component sample (*large orange component and small green component*) is injected into an open tube through which mobile phase flows laminarly with a parabolic flow profile. (*b*) The larger analyte remains near the center of the tube, preferentially experiencing the faster streamlines, whereas the smaller analyte experiences a slower average velocity through the tube because of its ability to sample slower streamlines near the tube walls. The black dotted circles circumscribing the analytes represent the hydrodynamic volume occupied by each analyte in solution. (*c*) Because of its faster average velocity through the tube, the larger analyte elutes from the tube earlier than the smaller analyte does. (*d*) Under laminar flow conditions, the interstitial medium of a packed column may be considered a collection of capillaries (tubes) in which HDC can be performed.

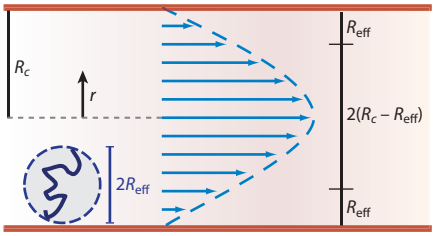

Figure 3

Definitions of the capillary radius R_c, the arbitrary position r in the capillary, the effective radius R_{eff} of the analyte, and the effective diameter $2(R_c - R_{eff})$ of the capillary for the analyte of effective radius R_{eff}.

smaller analytes, in addition to experiencing the faster streamlines, also experience the slower ones, thereby traveling through the tube (packed column) with a slower average velocity than that of their larger-sized counterparts. Therefore, larger analytes in the sample elute from the tube (packed column) earlier than smaller analytes do (**Figure 2*c***). Elution order in HDC is thus the same as in SEC (8): The larger analytes elute ahead of the smaller ones in both cases. The mechanisms of retention of these two techniques are different, however: In SEC, retention is due to preferential sampling of pore volume, whereas in HDC, it is due to preferential sampling of the streamlines of flow (or to a preferential distribution of analyte between fluid mechanical phases).

The migration behavior or retention mechanism of analytes in HDC has been described with various theoretical models. Because packed-column HDC can be considered a collection of intercommunicating capillaries, most of these theories have been derived from the model used to describe the migration of analytes in open capillaries during laminar flow. In general, migration behavior in HDC is described on the basis of a dilute solution rather than discrete particles because one can assume that colloidal forces, tubular pinch effects, and analyte-wall interactions are absent. For a fluid of density ρ and viscosity η flowing through an open tube (capillary) of radius R_c with an average velocity $\bar{u}$, laminarity is assumed for Reynolds numbers Re that are less than or equal to 2,000:

$$Re = \frac{2R_c\rho\bar{u}}{\eta}. \quad (1)$$

In a packed column, turbulence (nonlaminarity) manifests itself less suddenly and at lower Re than in an open tube, beginning gradually when Re is in the range of 1 to 100. The definition of Re in a packed column depends, however, not on the diameter of the column but on d_p, the diameter of the packing particles:

$$Re = \frac{d_p\rho\bar{u}}{\eta}. \quad (2)$$

On the basis of the above discussion, it is assumed that the parabolic flow profile is dominant and that the local velocity $u(r)$ for a position r in a flow channel of radius R_c (where $0 \leq r \leq R_c$; **Figure 3**) is given by

$$u(r) = 2\bar{u}\left[1 - \left(\frac{r}{R_c}\right)^2\right], \quad (3)$$

where the average velocity $\bar{u}$ is

$$\bar{u} = \frac{2}{R_c^2}\int_0^{R_c} u(r)dr \quad (4)$$

for point-like solutes (e.g., solvent molecules), which rapidly exchange between all available streamlines. The solvent molecules exit the column of length L after time t_m, given by

$$t_m = \frac{L}{\bar{u}}. \tag{5}$$

Conversely, the center of mass of non-point-like analytes of radius R_{eff} (i.e., analytes that are of actual interest in HDC) cannot sample the slower streamlines of the parabolic flow profile, namely those streamlines closest to the wall of the tube (**Figure 3**). For these larger analytes, the average velocity $\bar{u}_p$ is

$$\bar{u}_p = \frac{2}{(R_c - R_{\text{eff}})^2} \int_0^{R_c - R_{\text{eff}}} u(r) r dr, \tag{6}$$

and the average residence time t_p in the column is

$$t_p = \frac{L}{\bar{u}_p}. \tag{7}$$

The ratio of the effective analyte radius to the capillary radius is defined as the dimensionless parameter λ, which is also known as the aspect ratio of the analyte:

$$\lambda \equiv \frac{R_{\text{eff}}}{R_c}. \tag{8}$$

By combining Equations 3, 6, and 8, one obtains

$$\bar{u}_p = \bar{u}(1 + 2\lambda - \lambda^2). \tag{9}$$

From here, the dimensionless residence time τ of the analyte in the column can be defined as the ratio of the residence time of the analyte to that of a point-like solute:

$$\tau \equiv \frac{t_p}{t_m} = \frac{1}{1 + 2\lambda - \lambda^2}. \tag{10}$$

At this point, a question arises as to whether the diffusion process is sufficiently fast for the analyte to sample all available streamlines during a given transport process time t. To a first approximation, the answer comes in the form of a sufficiently large Fourier number Fo (which characterizes diffusion in time t over a characteristic length scale, in this case the capillary radius R_c or the effective capillary radius $R_c - R_{\text{eff}}$). The criteria are given by Equation 11 for point-like solutes and by Equation 12 for larger solutes (16):

$$Fo = \frac{D_m t}{R_c^2} \gg 1, \tag{11}$$

$$Fo = \frac{D_m t}{(R_c - R_{\text{eff}})^2} > 10, \tag{12}$$

where D_m is the diffusion coefficient of the solute.

Note, however, that even at $Fo > 200$ analytes may not always sample all streamlines to the extent predicted by theory (16), mainly because Equation 9 and, hence, Equation 10 are idealized equations in which the analyte is regarded as a nonrotating, impermeable hard sphere. Actually, the portion of the analyte in the region closest to the wall of the tube is located in a region of lower velocity than is the opposite side of the analyte. The resulting coupling of forces causes the analyte to rotate, thereby influencing its translational velocity. Additionally, analytes may have nonspherical shapes (e.g., ellipsoid or plate-like), may be permeable (e.g., composed of individual polymer molecules), or both. To account for these nonidealities, a modified quadratic term is

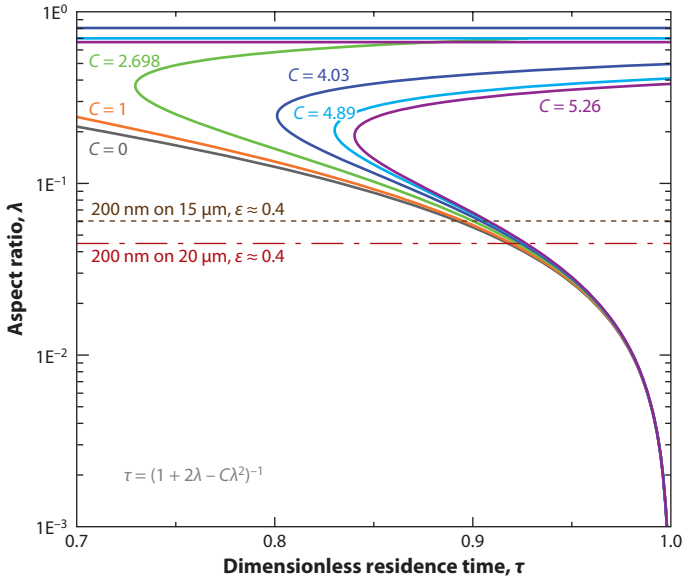

Figure 4

Relationship between aspect ratio λ and dimensionless residence time τ for various values of the quadratic modifier C in Equation 13 (see **Figure 6**). The light green curve corresponding to $C = 2.698$ is generally employed for dilute polymer solutions at thermodynamically good solvent and temperature conditions, whereas the light blue curve corresponding to $C = 4.89$ is generally employed for dilute suspensions of hard spheres. The dotted and dashed lines correspond to values of λ for an analyte with $R_{\text{eff}} = 200$ nm analyzed in a column of porosity $\varepsilon = 0.393$ and a particle diameter $d_p = 15$ μm (*brown dotted line*) or $d_p = 20$ μm (*red dashed line*).

introduced into Equation 10:

$$\tau = (1 + 2\lambda - C\lambda^2)^{-1}. \tag{13}$$

Various values of C have been proposed in the literature (10), each of which corresponds to a different model of HDC retention. For example, $C = 0$ corresponds to a highly idealized linear exclusion model that does not incorporate hydrodynamic effects, and $C = 1$ corresponds to a simple quadratic model, reflecting only the exclusion of the analyte center from the tube wall while taking into account the velocity profile. Other, more refined quadratic models have also been postulated to account for the added effects of analyte permeability and rotation. Each of these models has its own C value. Empirical evidence supports (*a*) the use of $C = 2.698$ for dilute polymer solutions at thermodynamically good solvent and temperature conditions and (*b*) a value of $C = 4.89$ for dilute suspensions of impermeable hard spheres.

Figure 4 plots the aspect ratio λ versus the dimensionless residence time τ for the various values of C corresponding to the linear and different quadratic models. This figure and the discussion leading up to it allow for several observations. First, it is possible to calculate, in theory, the size of the eluting species from the equations given above without resorting to a calibration curve. This calculation is done first by measuring τ. From the latter value, the aspect ratio λ is calculated. From this λ and knowledge of the tube radius R_c, the effective radius of the analyte R_{eff} is obtained. Although the relationship between R_{eff} and macromolecular radii such as the radius of gyration, the viscometric radius, the hydrodynamic radius, and the thermodynamic radius remains uncertain, the following approximation between R_{eff} and the radius of gyration R_G has often been used in the

literature (e.g., Reference 10):

$$R_{\text{eff}} \approx \frac{\sqrt{\pi}}{2} R_G. \tag{14}$$

Second, we observe that for τ values close to one, all the curves in **Figure 4** are quite steep; therefore, as $\tau \rightarrow 1$, the exact value of C is not particularly important. In this same region, however, the steepness of the curves means that a small error in τ leads to a large error in λ and, consequently, to a large error in the calculated size of the analyte. Third, as τ decreases, the slopes of the curves become less steep. In this region, exact knowledge of analyte conformation is needed to determine which value of C to use. Fourth, in the upper portion of the curves, which generally correspond to $\lambda > 0.2$, the quadratic term of Equation 13 is the leading term. The λ-versus-τ relationships in this region, however, lack any realistic physical meaning. Additionally, the concept of a particle with a radius that is approximately 20% that of the tube eluting in undisturbed Poiseuille flow is highly unlikely.

In the case of packed-column HDC, in calculations of λ and related parameters, the value of R_c to use is that of the so-called hydraulic radius of the column bed. The hydraulic radius may be considered the radius of a capillary with the same surface-to-volume ratio as the packed-column bed; it is defined as

$$R_c = \frac{d_p}{3} \frac{\varepsilon}{1-\varepsilon}, \tag{15}$$

where d_p is the diameter of the column packing particles and ε is the porosity of the column. For a column packed with nonporous spheres, the latter value is defined as

$$\varepsilon = \frac{V_{\text{void}}}{V_T} = \frac{4Ft_0}{\pi d^2 L}, \tag{16}$$

where V_{void} is the void volume of the column (which can be measured with a small analyte that is roughly equivalent in size to a solvent molecule) and V_T is the total volume of the empty column. The porosity can be calculated with the flow rate F, the void time t_0, the diameter d of the column, and the length L of the column. Calculation of ε for porous HDC columns is more ambiguous because the void volume corresponds to the elution volume of the smallest analyte that does not permeate into the pores of the packing material. As a rule of thumb, however, for most modern, commercially available, well-packed columns, porous or otherwise, $\varepsilon \approx 0.39$.

4. BAND BROADENING IN HYDRODYNAMIC CHROMATOGRAPHY

Due to space restrictions, our discussion of band broadening presupposes some knowledge of separation science and its terminology. As such, we begin with the expanded van Deemter equation and with the form to which this equation eventually reduces in HDC:

$$H = A + \frac{B}{u} + C_M u + C_{SM} u + C_S u, \tag{17a}$$

$$H = A + \frac{B}{u} + C_M u, \tag{17b}$$

where H represents plate height and u represents flow velocity. The A term corresponds to the contribution to band broadening from eddy dispersion, which arises from the multitude of pathways by which a molecule can find its way through a packed column. This term is generally considered to be either flow-velocity independent or weakly dependent. The B term, longitudinal diffusion, describes band broadening due to diffusion of analyte molecules through the column along the axis of the flow path. The contribution from this term increases with decreasing flow velocity because, all other factors being equal, at lower velocities the analyte spends a longer time

in the column and thus has more time to diffuse. The contribution from this term decreases with increasing analyte size and is, essentially, negligible for most macromolecules and particles in the size range shown in **Figure 1**, due to the small diffusion coefficient D_m of these analytes. *B*-term contributions to band broadening become manifest during the separation of small-sized, large-D_m analytes.

The *C* terms in Equation 17*a* correspond to various resistance to mass-transfer processes that may be encountered in different forms of column chromatography; the band-broadening contribution from each term is directly dependent upon flow velocity. The C_{SM} term represents the resistance to mass transfer provided by the stagnant mobile phase inside the pores of the column packing material. This term equals zero in both capillary and packed-column HDC (the contribution from C_{SM} to band broadening in HDC-SEC, that is, the contribution when both HDC and SEC are performed in the same porous packed column, is only to the peaks of analytes that elute in SEC mode, not to those that elute by HDC). The C_S term arises from resistance to mass transfer due to conventional liquid chromatographic sorptive processes. These processes, which are enthalpically dominated, should be (or can usually be made to be, through the addition of modifiers to the solvent/mobile phase) negligible because retention in ideal HDC is dominated by the solution translational entropy of the analyte, ΔS^{trans} (translation is between streamlines of flow, i.e., between different fluid mechanical phases). Here,

$$K_{\text{HDC}} \approx \exp\left(\Delta S^{\text{trans}}/R\right), \tag{18}$$

where K_{HDC} is the solute distribution coefficient and *R* is the gas constant. As such, $C_S \approx 0$ as well. For particulate-type analytes, which do not undergo the type of severe change in size as a function of temperature that can occur with polymers, the accuracy of this approximation can be checked by varying the temperature of the experiment and noting whether or not retention is essentially temperature independent. It should be, if $C_S \approx 0$.

The remaining resistance to the mass-transfer term in Equation 17*a* is C_M, the resistance to mass transfer due to mobile-phase effects in the interstitial medium. This is the region in which separation in packed-column HDC occurs, and as such, because $C_{SM} = 0$ and $C_S \approx 0$, C_M is the only mass-transfer term remaining in Equation 17*b*. Because the contribution to band broadening from C_M increases with increasing flow velocity, and on the basis of the above discussion of the relative contributions of the *A* and *B* terms to band broadening in HDC, Equation 17*b* predicts a linear increase in plate height with increasing flow velocity in high–flow rate regions, wherein the overall plate height should be dominated by the C_M term. Experimentally, however, this increase in plate height tapers off at high flow rates (8). This discrepancy is explained as follows.

The difference between the predicted and experimentally determined linear increases in band broadening with increasing flow velocity can be explained with the Giddings coupling theory. In this theory, both eddy diffusion and lateral diffusion effectively move solute molecules from one flow stream to another. Thus, the combination of both eddy and lateral diffusion provides a greater opportunity for analytes to experience different flow velocities (8, 13, 31). The result of the Giddings coupling theory is the harmonic combination of variances due to flow-path inequality and solute transfer in the mobile phase. The coupled sum results in reduced band broadening, compared with that from eddy diffusion alone.

The plate-height equation that incorporates the Giddings coupling theory for HDC can be expressed as

$$H = \frac{B}{u} + \frac{1}{\left(\frac{1}{A}\right) + \left(\frac{1}{C_M u}\right)}. \tag{19}$$

A more detailed description of this equation with respect to packing particle size d_p and solute-diffusion coefficient D_m is

$$H = b\frac{D_m}{u} + \frac{1}{\left(\frac{1}{ad_p}\right) + \left(\frac{D_m}{c_M u d_p^2}\right)}, \tag{20}$$

where a, b, and c_M are the coefficients of the respective dispersion terms in the plate-height equation.

Clearly, band broadening in ideal HDC is determined exclusively by longitudinal diffusion and extraparticle effects. Because the latter are a result of convective mixing through the type of coupling mechanism described above, in packed-column HDC, plate height is given by (10, 17, 32)

$$H = \underbrace{b\frac{D_m}{u}}_{\substack{\text{Longitudinal}\\ \text{diffusion}\\ \text{effects}}} + \underbrace{\frac{d_p}{\left(\frac{D_m}{ud_p} + \frac{1}{1.4}\right)}}_{\substack{\text{Convective}\\ \text{mixing}\\ \text{effects}}}, \tag{21}$$

where b is a constant with a value of 1.2 to 1.4. The first term in Equation 21 describes the longitudinal diffusion of the analyte, and the second term depicts the effects of convective mixing on dispersions. As noted above, in HDC of macromolecules and particles, the longitudinal diffusion term is typically very small compared with the convective mixing term because of the small diffusion coefficients of these analytes. Convective mixing, the dominating band-broadening term, is a result of unsteady diffusion across the analyte-solvent concentration gradients in the capillary channels (33). Per Equation 21, at higher solvent velocities $H \approx 1.4d_p$.

For a more universal representation of band broadening and column efficiency, it is convenient to represent the plate height–versus–flow velocity relationship in terms of dimensionless quantities. Reduced plate height h, used to compare the efficiency of columns with different particle sizes, is defined as

$$h = \frac{H}{d_p}, \tag{22}$$

and reduced velocity ν is defined as

$$\nu = \frac{ud_p}{D_m}. \tag{23}$$

In HDC, h is virtually independent of λ and of ν, for $\nu_{\mathrm{HDC}} > 5$ (13). In terms of the dimensionless parameters h and ν, band broadening in HDC is described as

$$h = \frac{b}{\nu} + \frac{1}{\left(\frac{1}{\nu} + \frac{1}{1.4}\right)}. \tag{24}$$

In accordance with the conclusions drawn from Equation 21, Equation 24 dictates that at higher values of ν, $h \approx 1.4$. This result is depicted in **Figure 5**, where the relationship between h and ν for HDC is plotted as a single, λ-independent plate-height curve (where the intermediate value of $b = 1.3$ was chosen) in which $h_{\mathrm{HDC}} \approx 1.4$ at all but the lowest ν. This result implies that, in HDC, the highest rate of generating theoretical plates is achieved when the reduced velocity is as high as possible and that the analysis speed can be increased significantly without influencing either the number of theoretical plates or chromatographic resolution.

Although **Figure 5** indicates that there is no realistic upper limit to the flow velocity at which HDC separations may be conducted, at least with respect to band-broadening considerations,

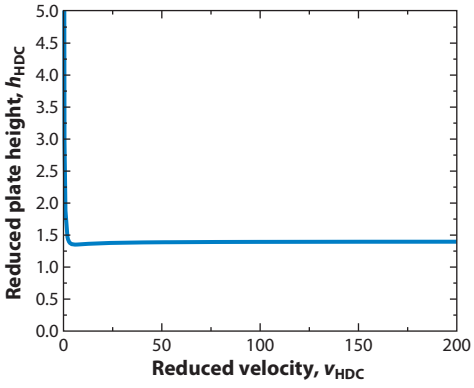

Figure 5

Reduced plate height h versus reduced velocity ν for packed-column hydrodynamic chromatography (HDC), based on Equation 24, where $b = 1.3$. Over a broad range of ν values, $h_{HDC} \approx 1.4$.

such a limit may be imposed for many different reasons. First is the possibility of on-column, flow-induced degradation of large analytes, especially ultrahigh-M polymers, which arises from the high shear rates to which these analytes are exposed in the interstitial medium of a packed column. This shear rate $\dot{\gamma}$ is given by (34, 35)

$$\dot{\gamma} = \frac{4F}{\varepsilon A R_c}, \tag{25}$$

where A is the cross-sectional area of the column; F is the volumetric flow rate; and the hydraulic radius R_c and porosity ε are defined as per Equations 15 and 16, respectively. Second is the possibility of no longer operating in HDC mode because, with increasing flow rate, the mechanism of separation has shifted to that of SC. Such HDC-to-SC transitions are discussed more fully in Section 8.2. The third limitation on flow velocity concerns the back-pressure P limits of the physical system for separations in columns packed with small-diameter particles. Because $P \propto \frac{1}{d_p^2}$, this limitation becomes especially important for the type of ultrahigh-pressure HDC separations that use sub-2-μm-diameter particles, which have recently been reported in the literature (36). (Also, the aforementioned possibility of on-column, flow-induced degradation is of increased concern in this situation, as $\dot{\gamma} \propto \frac{1}{d_p}$.) The last consideration for HDC flow velocity is the possibility of Taylor dispersion effects occurring during the separation. Such effects, which are discussed in detail in Reference 33, may actually result in a slight band narrowing at higher flow rates (24). Because of the relatively minor impact of these effects, they are not discussed further here.

5. RESOLUTION IN HYDRODYNAMIC CHROMATOGRAPHY

Chromatographic resolution R_s in HDC is given by (11)

$$R_s = (\alpha - 1) \cdot (1 - C\lambda)\lambda\tau\sqrt{N} \tag{26}$$

for two solutes with a small difference in τ; the term α corresponds to the ratio of the R_{eff} of these solutes (i.e., $\alpha = R_{eff,1}/R_{eff,2}$), so that $\Delta\lambda/\lambda = \alpha - 1$. N is the plate count of the system, defined as $N = L/H$, where L is the column length. The terms H, C, λ, and τ retain the same meanings as above.

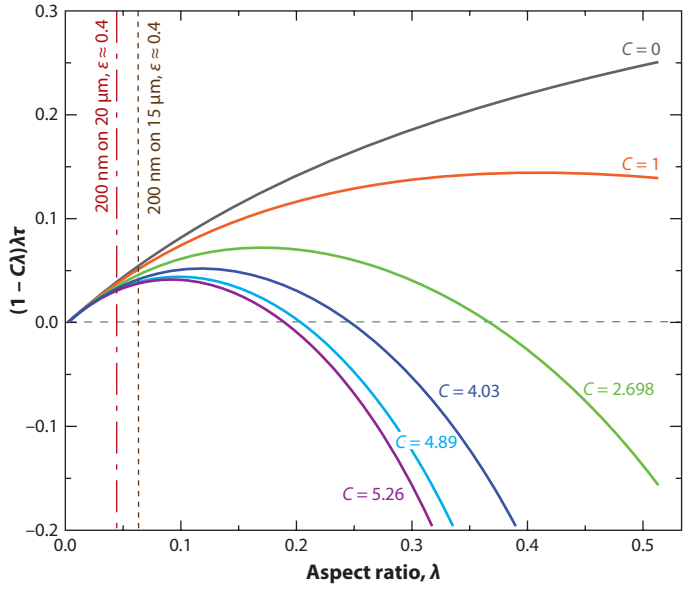

Figure 6

Plot of retention factor $(1 - C\lambda)\lambda\tau$ in resolution (Equation 26) versus aspect ratio λ for different values of the quadratic modifier C from Equation 13 (see **Figure 4**). Values of λ are shown for an analyte with $R_{\text{eff}} = 200$ nm analyzed with a column of porosity $\varepsilon = 0.393$ and a particle diameter $d_p = 15$ μm (*brown dotted line*) or $d_p = 20$ μm (*red dashed line*).

Equation 26 contains a selectivity term $(\alpha - 1)$, a kinetic term $\sqrt{N}$, and a retention term $(1 - C\lambda)\lambda\tau$. The role of the aspect ratio λ in retention and, consequently, resolution is nontrivial, as shown in **Figure 6**, where the retention term of the resolution equation is plotted versus λ for various values of the quadratic modifier C (Equation 13) (**Figure 4**). First, the pure exclusion model of HDC retention, where $C = 0$, is not realistic and coincides only with the other models being plotted (which include permeability and/or rotation effects, inter alia) at very small λ, where R_s is small. Second, **Figure 6** shows that, at given α and N, the choice of capillary or packed-column R_c is crucial to obtaining reasonable values of R_s. For packed-column HDC, as seen from Equation 15, one can vary R_c discretely by choosing columns that differ from one another in diameter of packing material d_p.

The dependence of R_s on λ and τ (the latter through choice of the quadratic modifier C) is shown in **Figures 4** and **6** for an analyte with $R_{\text{eff}} = 200$ nm analyzed on two individual packed columns: One has $d_p = 15$ μm ($\lambda = 0.062$), the other has $d_p = 20$ nm ($\lambda = 0.046$), and both have porosity $\varepsilon = 0.393$. As λ becomes larger—which, for a given analyte at a given set of experimental conditions, corresponds to a smaller R_c arising from a smaller d_p—the choice of model becomes more important when trying to derive size information from first principles. However, the slope of the curves in **Figure 6** decreases with increasing λ (up to $\lambda \approx 0.1$ for $C = 5.26$ and up to $\lambda \approx 0.18$ for $C = 2.698$, which correspond, respectively, to the hard sphere and dilute polymer solution models). This decrease signifies that R_s increases with decreasing d_p, all other factors being equal and given the parenthetical upper limits of λ just mentioned. Some caveats regarding the choice of columns with small d_p are given at the end of Section 4.

Packed-column HDC for colloidal and ultrahigh-M polymer separations is not a particularly high-resolution technique. However, to a limited extent, the multidetector approach described

in Section 6 overcomes this issue in the analysis of bi-, tri-, and tetramodal blends of PS and poly(methyl methacrylate) latexes (25). This advantage comes from (*a*) the ability, conferred by so-called absolute detectors such as MALS and QELS, to determine the size of each component in the blend and the change in size across the blend and (*b*) the dependence of detector response on the combined M and chemical identity of each blend component.

6. MULTIDETECTOR PACKED-COLUMN HYDRODYNAMIC CHROMATOGRAPHY

6.1. Particle Characterization

Until recently, most work on particle sizing via HDC employed a single, concentration-sensitive detector, and the particle sizes and distributions were derived through the application of calibration curves constructed with standards that bore little, if any, architectural and/or chemical resemblance to the analytes themselves. The accuracy of this type of approach is suspect at best, and the information obtained is fairly limited. The recent introduction of triple- and quadruple-detector HDC approaches involves the following detection methods (23–29): MALS, QELS (also known as dynamic light scattering), VISC, and DRI. Through various combinations of these detection methods, the following information can be obtained.

1. The MMD and associated statistical moments, using MALS and DRI.
2. The distributions and associated statistical moments of the following size parameters:
   a. The radius of gyration (R_G), using MALS-DRI;
   b. The hydrodynamic (Stokes) radius (R_H), using QELS-DRI;
   c. The viscometric radius (R_η), using MALS-VISC-DRI;
   d. The shape and compactness of the sample, through the dimensionless parameter $\rho \equiv R_{G,z}/R_{H,z}$, obtained with MALS-QELS (8, 23, 37); and
   e. The structure and compactness of the sample, through the dimensionless ratio $R_{\eta,w}/R_{G,z}$, obtained using MALS-VISC-DRI (8, 28, 38–40).

Because each detector analyzes the eluate in continuous fashion, the multidetector approach allows one to obtain the mutual interdependence of size, molar mass, shape, structure, and compactness continuously across the elution profile of the sample, in a single analysis.

Figure 7 illustrates how HDC with online MALS, QELS, VISC, and DRI detection was employed in the analysis of a nanocage drug-delivery vesicle (26). The chromatogram represents the elution profile as monitored by the 90° photodiode of the MALS detector. As the sample becomes smaller in size, its molar mass increases, which indicates that the sample becomes more compact as a function of decreasing size. As the sample becomes more compact, its shape transitions from that of a prolate ellipsoid (for which ρ ranges from 1.36 to 2.24, depending on the axial ratio of the ellipsoid) to that of a sphere whose density is intermediate between that of a hard sphere and that of a soft sphere (for which $\rho = 0.778$ and 0.977, respectively). Use of a VISC detector allowed for determination of the viscometric radius R_η of the vesicle, and use of a DRI detector permitted calculation of the statistical moments associated with M, R_G, R_H, and R_η (8).

6.2. Ultrahigh-*M* Polymer Characterization

The use of dual-detector HDC for characterizing ultrahigh-M polymers is described in Section 2. The triple-detector approach (MALS-QELS-DRI or MALS-VISC-DRI) has recently been extended to this class of analytes as well. To date, most applications of multidetector HDC

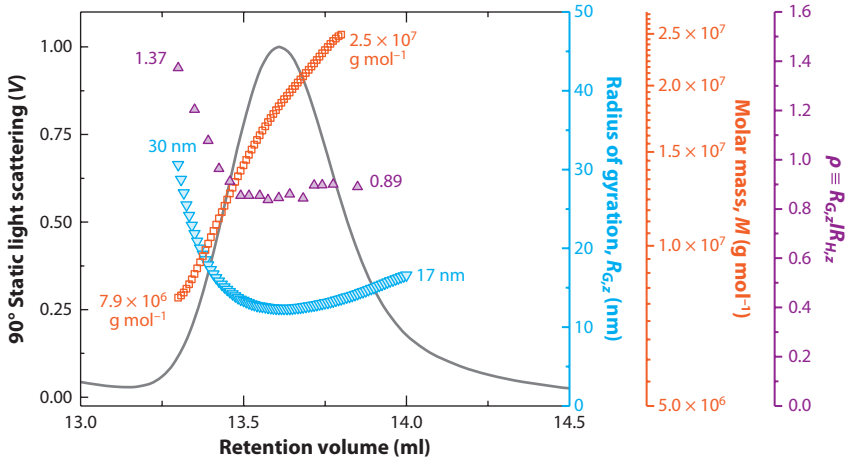

Figure 7

Characterization of the molar mass, size, shape, and structure of a nanocage drug-delivery vesicle by hydrodynamic chromatography (HDC), multiangle static light scattering (MALS), quasi-elastic light scattering, and differential refractometry. The solid gray line corresponds to an HDC chromatogram, as monitored by a 90° photodiode of the MALS detector. The upside-down blue triangles correspond to the radius of gyration R_G. The open orange squares correspond to molar mass M. The purple triangles correspond to the dimensionless ratio ρ. See Reference 26 for details and for the distribution of R_H.

in the polymeric arena have been to polysaccharides such as alternan (the analysis of which is described below) and to the starch components amylose and amylopectin (20, 24, 41).

Due to the interstitial and, especially, at- and through-pore stresses that accumulate on polymers during their passage through the packed, porous medium of SEC columns (34, 35, 42), very low flow rates must be employed to avoid degradation during SEC analysis, which lengthens run times to several hours. Even under these extreme conditions, large polymers can degrade in SEC, rendering accurate characterization with this technique impossible (24, 35). Because analytes experience no pore stresses in HDC (only interstitial stresses, as described by Equation 25), this gentler method can provide a means by which to analyze polymers that cannot be characterized accurately by SEC or to characterize ultrahigh-M polymers in a fraction of the time needed to do so by SEC. Similar information to that obtained for particulate-type analytes, described in the previous section, can be obtained for polymers through multidetector HDC.

Figure 8*a* shows the elution profiles of the polysaccharide alternan ($M_w \approx 5 \times 10^7$ g mol^{-1}), when this biopolymer was analyzed by HDC-MALS-VISC-DRI and by SEC-MALS-DRI. **Figure 8*b*** shows the MMDs obtained by each technique (24). Analysis by SEC was conducted at 0.2 ml min^{-1} [note that flow rates as low as 0.05 ml min^{-1} did not yield more accurate results (35)] with columns that had a large particle size and a large pore size. In other words, the analysis was optimized to minimize on-column, flow-induced degradation based on commercially available column technology. Even under such mild conditions, degradation of this alternan sample was evident in SEC, as indicated by the fact that the M_w and $R_{G,z}$ values obtained by SEC-MALS-DRI were substantially lower than those obtained by off-line MALS, that is, when the photometer was decoupled from the separation system. Conversely, HDC analysis was accomplished in a fraction (less than one-fifteenth) of the time needed for SEC analysis; the M_w and $R_{G,z}$ obtained were remarkably similar to the off-line MALS values; and consequently, as shown in **Figure 8*b***, the MMD of the polysaccharide extended to higher molar masses when determined by HDC compared with

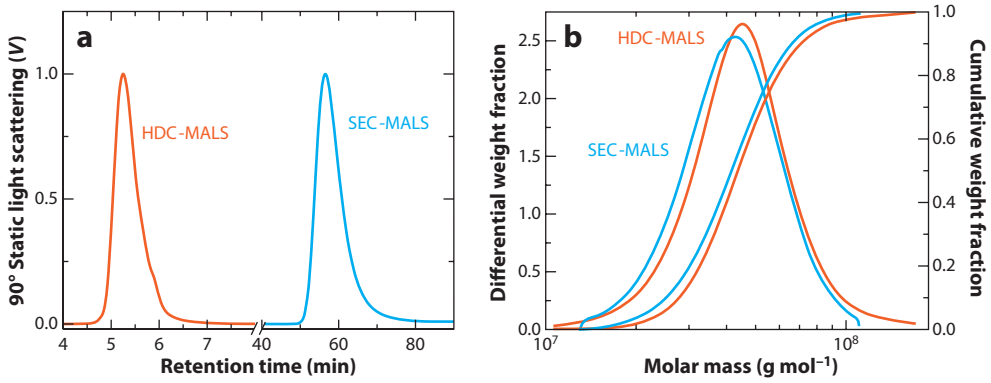

Figure 8

Multidetector hydrodynamic chromatography (HDC) and size-exclusion chromatography (SEC) analysis of the ultrahigh-*M* polysaccharide alternan. (*a*) Elution profiles, as monitored by the 90° multiangle light scattering (MALS) photodiode, for HDC (*orange*) and SEC (*blue*) analysis. (*b*) Differential and cumulative molar mass distributions, as determined by HDC-MALS (*orange*) and SEC-MALS (*blue*). See Reference 24 for details.

SEC under otherwise identical conditions. Incorporation of the VISC detector into HDC allowed for determination of the intrinsic viscosity $[\eta]$ and of R_η. Comparison between these values for alternan and the values both measured and calculated for the linear polysaccharide pullulan yielded strong evidence for the large amount of long-chain branching in alternan. The long-chain branching affords alternan a highly compact conformation in solution and, consequently, much lower values of $[\eta]$ and R_η compared with the nonbranched pullulan.

In the above cases, very small pore SEC columns are often used; these columns have pores that are substantially smaller than the solvated size of the polymer or particle. Therefore, from the point of view of the analyte, the column packing material may be regarded as, essentially, nonporous. In broadly polydisperse samples, however, the porous packing material may have a pore size such that the smaller part of the sample separates within the column through a size-exclusion mechanism, whereas the larger components in the sample separate through an HDC mechanism. This type of analysis, termed HDC-SEC, has been employed by Rolland-Sabaté et al. (41) to determine the *M* and size distribution of native starches and by Uliyanchenko et al. (36) in ultrahigh-pressure liquid chromatography studies of PSs.

7. MICROCAPILLARY HYDRODYNAMIC CHROMATOGRAPHY

Although single-detector (chiefly UV) capillary HDC commercial instruments have not met with much acceptance in the particle-sizing arena due to the difficulty of applying the technique to non-PS latexes, microcapillary HDC has recently experienced success in analyses of DNA and DNA fragments, where it is sometimes referred to as free-solution HDC. The literature on microcapillary HDC of polymers and particles through the mid 1990s, which employed capillaries up to 10 μm in diameter, is reviewed in Reference 16. Recent work on wide-bore HDC, which employs capillaries up to 400 μm in diameter, is reviewed in Reference 43.

The capillaries used for modern bioanalytical work usually have internal diameters between 1 and 5 μm and lengths between 0.75 and 15 m. The detection method of choice is normally laser-induced fluorescence (LIF). Application of HDC-LIF to the separation and analysis of DNA and DNA fragments helps obviate many of the issues with techniques such as capillary and gel

LIF: laser-induced fluorescence

electrophoresis, which include low mass-detection efficiency and a narrow dynamic range for DNA sizing (44, 45).

Performing HDC in a 2.5 μm × 445 cm capillary, Wang et al. (44) recently separated DNA fragments ranging from 75 base pairs to 106,000 base pairs. Liu et al. (45) used microcapillary HDC to perform single-molecule analysis with only 5 pl of sample and 240 ymol (~150 molecules) of DNA.

8. HYDRODYNAMIC, SIZE-EXCLUSION, AND SLALOM CHROMATOGRAPHY

This section discusses the possibility of HDC effects manifesting themselves during SEC analysis and of SC effects manifesting themselves during HDC analysis. A more detailed discussion may be found in sections 2.6.3 and 2.6.4 of Reference 8. Results of recent experiments in this area are given in Reference 36.

8.1. Hydrodynamic Chromatographic Effects in Size-Exclusion Chromatography

Under appropriate conditions, HDC effects may manifest themselves during the course of an SEC separation, even in the case of analytes whose solvated size is smaller than the size of the pores in the column packing material. Manifestation of these effects depends on flow rate, aspect ratio λ, and the ratio of pore diameter R_p to particle diameter d_p.

Studies have indicated than a ratio of R_p to d_p of less than 0.002 leads to negligible HDC effects in SEC (12). However, in most SEC columns this ratio greatly exceeds 0.002. Once in HDC mode, however, selectivity depends on λ. On the basis of Equation 13, an analyte with $\lambda = 0.005$ has a retention time $t_p = 0.99t_m$, where t_m is the retention time of the solvent (Equation 5), which results in the likely coelution of these two species. For HDC effects to become noticeable in SEC, a useful rule of thumb is that λ should be greater than 0.02.

When dealing with hard spheres and other nondeformable analytes, concerns regarding flow-induced deformation are nonexistent. This is not so in the case of polymers and deformable particles. The shape that these types of analytes adopt in solution and, consequently, their size, is the result of an equilibrium between the randomizing forces of Brownian motion and the deforming forces imposed by the hydrodynamics of solvent flow. This equilibrium is given by the Deborah number *De*:

$$De = k\frac{\bar{v}}{d_p}\frac{6.12\Phi\eta_0 R_G^3}{RT}, \tag{27}$$

where k is a constant that depends on the structure of the flow channels (usually, $k = 6$), $\bar{v}$ is the superficial solvent velocity, Φ is Flory's constant after correction for non-θ solvent and temperature conditions, η_0 is the viscosity of the neat solvent, T is the absolute temperature, and all the other symbols retain the same meanings as above. At $De < 0.1$, polymer stretching is essentially insignificant, and the analyte retains the same shape and size as at equilibrium conditions. At $De = 0.1$, the onset of stretching occurs. As such, HDC effects manifest themselves in SEC when $0.1 \leq De < 0.5$; these effects become noticeable at $\lambda > 0.02$, as described above.

8.2. Slalom-Chromatographic Effects in Hydrodynamic Chromatography

The previous section discussed what occurs when $De < 0.5$. When $De \geq 0.5$, hydrodynamic forces prevail over Brownian motion, and macromolecules undergo a critical coil-to-stretch transition

that leads to highly extended, thread-like structures that must turn frequently around the column packing particles during their passage through the tortuous interstitial channels. Said repetitive, continuous turning retards elution relative to the HDC elution of macromolecules at equilibrium conditions. In this so-called SC mode, longer polymers elute later than do shorter ones, and the elution order is therefore the opposite of that in HDC. For broadly disperse polymers, the smaller species in the sample may not be large enough to undergo a coil-to-stretch transition and, consequently, elute in HDC mode, whereas larger polymers elute in SC mode. Online monitoring of molar mass in conjunction with size [by, e.g., MALS detection (21, 22)] across the elution profile and as a function of flow rate is the most accurate way to determine whether an HDC-to-SC transition has occurred. In general, as shown in Equation 27, SC effects in HDC can usually be avoided by making the proper choice of solvent and temperature conditions (with respect to both the viscosity of the solvent and the thermodynamic state of the dilute polymer solution), flow rate, and size of the column packing material (with respect to the solvated size of the polymer, as given by R_G).

9. CONCLUSIONS

Aided by the power of multiple detection, packed-column HDC appears to have finally come of age. Limitations to the technique certainly exist, most notably relatively low chromatographic resolution and the possibility for degradation of very large and fragile macromolecules. However, the ability to determine the mutual interdependence of molar mass, size, shape, and structure of particulate and polymeric analytes in a single, rapid analysis by use of instrumentation common to most macromolecular separations laboratories, without necessitating a large capital outlay for additional hardware, affords HDC a unique advantage over other particle-sizing and macromolecular characterization methods. Although obtaining information about analyte size and size distribution, from first principles, remains a model-dependent approach, this obstacle can be overcome through online detection methods such as MALS, QELS, and/or VISC in conjunction with a concentration-sensitive detector (e.g., a differential refractometer). Additionally, the large separation power and low sample consumption inherent to microcapillary HDC are already establishing this technique among the large arsenal of bioanalytical methods.

DISCLOSURE STATEMENT

The authors are not aware of any affiliations, memberships, funding, or financial holdings that might be perceived as affecting the objectivity of this review. Commercial products are identified to adequately specify the experimental procedure. Such identification does not imply endorsement or recommendation by the National Institute of Standards and Technology, nor does it imply that the materials identified are necessarily the best available for the purpose.

LITERATURE CITED

1. Brewer AK. 2010. *Multi-detector hydrodynamic chromatography: particle characterization and ultra-high molar mass polymer analysis*. PhD thesis, Florida State Univ. 167 pp.
2. Lespes G, Gigault J. 2011. Hyphenated analytical techniques for multidimensional characterization of submicron particles: a review. *Anal. Chim. Acta* 692:26–41
3. Pedersen KO. 1962. Exclusion chromatography. *Arch. Biochem. Biophys. Suppl.* 1:157–68
4. DiMarzio EA, Guttman CM. 1969. Separation by flow. *Polym. Lett.* 7:267–72
5. DiMarzio EA, Guttman CM. 1970. Separation by flow. *Macromolecules* 3:131–46

6. DiMarzio EA, Guttman CM. 1970. Separation by flow. II. Application to gel permeation chromatography. *Macromolecules* 3:681–91
7. DiMarzio EA, Guttman CM. 1971. Separation by flow and its application to gel permeation chromatography. *J. Chromatogr.* 55:83–97
8. Striegel AM, Yau WW, Kirkland JJ, Bly DD. 2009. *Modern Size-Exclusion Liquid Chromatography*. New York: Wiley. 494 pp. 2nd ed.
9. Small H. 1974. Hydrodynamic chromatography. A technique for size analysis of colloidal particles. *J. Colloid Interface Sci.* 48:147–61
10. Tijssen R, Bos J, van Kreveld ME. 1986. Hydrodynamic chromatography of macromolecules in open capillary tubes. *Anal. Chem.* 58:3036–44
11. Kraak JC, Oostervink R, Poppe H, Esser U, Unger KK. 1989. Hydrodynamic chromatography of macromolecules on 2 μm non-porous spherical silica gel packings. *Chromatographia* 27:585–90
12. Stegeman G, Kraak JC, Poppe H. 1991. Hydrodynamic and size-exclusion chromatography of polymers on porous particles. *J. Chromatogr.* 550:721–39
13. Stegeman G, Kraak JC, Poppe H. 1993. Dispersion in packed-column hydrodynamic chromatography. *J. Chromatogr.* 634:149–59
14. Stegeman G, Kraak JC, Poppe H, Tijssen R. 1993. Hydrodynamic chromatography of polymers in packed columns. *J. Chromatogr.* 657:283–303
15. Stegeman G, van Asten AC, Kraak JC, Poppe H, Tijssen R. 1994. Comparison of resolving power and separation time in thermal field-flow fractionation, hydrodynamic chromatography, and size-exclusion chromatography. *Anal. Chem.* 66:1147–60
16. Bos J, Tijssen R. 1995. Chapter 4: Hydrodynamic chromatography of polymers. In *Chromatography in the Petroleum Industry*, ed. ER Adler, pp. 95–126. Amsterdam: Elsevier
17. Venema E, Kraak JC, Poppe H, Tijssen R. 1996. Packed-column hydrodynamic chromatography using 1-μm non-porous silica particles. *J. Chromatogr. A* 740:159–67
18. Langhorst MA, Stanley FW Jr, Cutié SS, Sugarman JH, Wison LR, et al. 1986. Determination of nonionic and partially hydrolyzed polyacrylamide molecular weight distributions using hydrodynamic chromatography. *Anal. Chem.* 58:2242–47
19. von Wald G, Langhorst M. 1991. Chapter 20: Viscometry as a detection scheme for particles in separation techniques for particle distribution analysis. In *Particle Size Distribution II: Assessment and Characterization*, ed. T Provder, pp. 308–23. Washington, DC: Am. Chem. Soc.
20. Klavons JA, Dintzis FR, Millard MM. 1997. Hydrodynamic chromatography of waxy maize starch. *Cereal Chem.* 74:832–36
21. Liu Y, Radke W, Pasch H. 2005. Coil-stretch transition of high molar mass polymers in packed-column hydrodynamic chromatography. *Macromolecules* 38:7476–84
22. Liu Y, Radke W, Pasch H. 2006. Onset of the chromatographic mode transition from hydrodynamic chromatography to slalom chromatography: an effect of polymer stretching. *Macromolecules* 39:2004–6
23. Brewer AK, Striegel AM. 2009. Particle size characterization by quadruple-detector hydrodynamic chromatography. *Anal. Bioanal. Chem.* 393:295–302
24. Isenberg SL, Brewer AK, Côté GL, Striegel AM. 2010. Hydrodynamic versus size exclusion chromatography characterization of alternan and comparison to off-line MALS. *Biomacromolecules* 11:2505–11
25. Brewer AK, Striegel AM. 2010. Hydrodynamic chromatography of latex blends. *J. Sep. Sci.* 33:3555–63
26. Brewer AK, Striegel AM. 2011. Characterizing a spheroidal nanocage drug delivery vesicle using multidetector hydrodynamic chromatography. *Anal. Bioanal. Chem.* 399:1507–14
27. Brewer AK, Striegel AM. 2011. Characterizing the size, shape, and compactness of a polydisperse prolate ellipsoidal particle via quadruple-detector hydrodynamic chromatography. *Analyst* 136:515–19
28. Brewer AK, Striegel AM. 2011. Characterizing string-of-pearls colloidal silica by multidetector hydrodynamic chromatography and comparison to multidetector size-exclusion chromatography, off-line multiangle static light scattering, and transmission electron microscopy. *Anal. Chem.* 83:3068–75
29. Striegel AM. 2012. Hydrodynamic chromatography: packed columns, multiple detectors, and microcapillaries. *Anal. Bioanal. Chem.* 402:77–81
30. McHugh AJ. 1984. Particle size measurement using chromatography. *Crit. Rev. Anal. Chem.* 15:63–117

31. Giddings CJ. 1965. *Dynamics of Chromatography: Principles and Theory*. New York: Marcel Dekker. 340 pp.
32. Venema E, de Leeuw P, Kraak JC, Poppe H, Tijssen R. 1997. Polymer characterization using on-line coupling of thermal field flow fractionation and hydrodynamic chromatography. *J. Chromatogr. A* 765:135–44
33. Probstein RF. 1994. *Physicochemical Hydrodynamics: An Introduction*. Boston: Butterworths. 353 pp.
34. Striegel AM. 2007. Observations regarding on-column, flow-induced degradation during SEC analysis. *J. Liq. Chromatogr. Rel. Technol.* 31:3105–14
35. Striegel AM, Isenberg SL, Côté GL. 2009. An SEC/MALS study of alternan degradation during size-exclusion chromatographic analysis. *Anal. Bioanal. Chem.* 394:1887–93
36. Uliyanchenko E, Schoenmakers PJ, van der Wald S. 2011. Fast and efficient size-based separations of polymers using ultra-high-pressure liquid chromatography. *J. Chromatogr. A* 1218:1509–18
37. Burchard W. 1999. Solution properties of branched macromolecules. *Adv. Polym. Sci.* 143:113–94
38. Ostlund SG, Striegel AM. 2008. Ultrasonic degradation of poly(γ-benzyl-L-glutamate), and archetypal highly extended polymer. *Polym. Degrad. Stab.* 93:1510–14
39. Haidar Ahmad I, Striegel DA, Striegel AM. How does sequence length heterogeneity affect the dilute solution conformation of copolymers? *Polymer* 52:1268–77
40. Roovers J. 1999. Dilute solution properties of regular star polymers. In *Star and Hyperbranched Polymers*, ed. MK Mishra, S Kobayashi, pp. 285–341. New York: Marcel Dekker
41. Rolland-Sabaté A, Guilois S, Jaillais B, Colonna P. 2011. Molecular size and mass distributions of native starches using complementary separation methods: asymmetrical flow field flow fractionation (A4F) and hydrodynamic and size exclusion chromatography (HDC-SEC). *Anal. Bioanal. Chem.* 399:1493–505
42. Barth HG, Carlin FJ Jr. 1984. A review of polymer shear degradation in size-exclusion chromatography. *J. Liq. Chromatogr. Rel. Technol.* 7:1717–38
43. Okada T. 2010. Hydrodynamic chromatography in narrow and wide bores: whether radial diffusion is essential or not. *J. Liq. Chromatogr. Rel. Technol.* 33:1116–29
44. Wang X, Veerappan V, Cheng C, Jiang X, Allen RD, et al. 2010. Free solution hydrodynamic separation of DNA fragments from 75 to 106,000 base pairs in a single run. *J. Am. Chem. Soc.* 132:40–41
45. Liu KJ, Rane TD, Zhang Y, Wang T-H. 2011. Single-molecule analysis enables free solution hydrodynamic separation using yoctomole levels of DNA. *J. Am. Chem. Soc.* 133:6898–901

Annual Review of
Analytical Chemistry

Volume 5, 2012

Contents